

Regulation of *ITGA3* by the anti-tumor *miR-199* family inhibits cancer cell migration and invasion in head and neck cancer

Keiichi Koshizuka,^{1,2} Toyoyuki Hanazawa,² Naoko Kikkawa,² Takayuki Arai,¹ Atsushi Okato,¹ Akira Kurozumi,¹ Mayuko Kato,¹ Koji Katada,² Yoshitaka Okamoto,² and Naohiko Seki¹

Departments of ¹Functional Genomics; ²Otorhinolaryngology/Head and Neck Surgery, Chiba University Graduate School of Medicine, Chiba, Japan

Key words

Anti-tumor, head and neck squamous cell carcinoma, *ITGA3*, *miR-199a*, *miR-199b*

Correspondence

Naohiko Seki, Associate Professor of Functional Genomics, Department of Functional Genomics, Chiba University Graduate School of Medicine, 1-8-1 Inohana Chuo-ku, Chiba 260-8670, Japan.
Tel: +81-43-226-2971; Fax: +81-43-227-3442;
E-mail: naoseki@faculty.chiba-u.jp

Funding Information

JSPS KAKENHI, 16K20229, 15K10801, 25462676 and 26462596

Received February 28, 2017; Revised June 1, 2017;
Accepted June 8, 2017

Cancer Sci 108 (2017) 1681–1692

doi: 10.1111/cas.13298

For patients with head and neck squamous cell carcinoma (HNSCC), survival rates have not improved due to local recurrence and distant metastasis. Current targeted molecular therapies do not substantially benefit HNSCC patients. Therefore, it is necessary to use advanced genomic approaches to elucidate the molecular mechanisms underlying the aggressiveness of HNSCC cells. Analysis of our microRNA (miRNA) expression signature by RNA sequencing showed that the *miR-199* family (*miR-199a-5p*, *miR-199a-3p*, *miR-199b-5p* and *miR-199b-3p*) was significantly reduced in cancer tissues. Ectopic expression of mature miRNA demonstrated that all members of the *miR-199* family inhibited cancer cell migration and invasion by HNSCC cell lines (SAS and HSC3). These findings suggested that both passenger strands and guide strands of miRNA are involved in cancer pathogenesis. *In silico* database and genome-wide gene expression analyses revealed that the gene coding for integrin $\alpha 3$ (*ITGA3*) was regulated by all members of the *miR-199* family in HNSCC cells. Knockdown of *ITGA3* significantly inhibited cancer cell migration and invasion by HNSCC cells. Moreover, overexpression of *ITGA3* was confirmed in HNSCC specimens, and high expression of *ITGA3* predicted poorer survival of the patients ($P = 0.0048$). Our data revealed that both strands of pre-*miR-199a* (*miR-199a-5p* and *miR-199a-3p*) and pre-*miR-199b* (*miR-199b-5p* and *miR-199b-3p*) acted as anti-tumor miRNA in HNSCC cells. Importantly, the involvement of passenger strand miRNA in the regulation of cellular processes is a novel concept in RNA research. Novel miRNA-based approaches for HNSCC can be used to identify potential targets for the development of new therapeutic strategies.

Head and neck squamous cell carcinoma (HNSCC) develops in the mucous membranes of the nasopharynx, oral cavity, oropharynx, larynx and hypopharynx.⁽¹⁾ Due to local recurrence and distant metastasis, the 5-year survival frequency of patients with HNSCC has not improved for 20 years.^(2–5) Recently, new targeted therapeutics have been developed to inhibit oncogenic receptor-mediated signaling, including that in HNSCC.⁽⁶⁾ However, these targeted therapies have offered few benefits in the management of patients with disease recurrence and distant metastasis.^(6,7) Therefore, there is a need for new and effective treatment options based on genome-wide RNA networks analyses.

MicroRNA (miRNA) belong to a family of small non-coding RNA.⁽⁸⁾ miRNA fine-tune the expression of protein coding/noncoding RNA by repressing translation or cleaving RNA transcripts in a sequence-dependent manner.^(8–10) The discovery of miRNA has suggested new approaches to cancer therapeutics. A unique characteristic of miRNA is that a single miRNA regulates a large number of RNA transcripts in human cells.^(11,12) Therefore, the presence of dysregulated miRNA can disturb entire RNA networks. Numerous studies have

shown that miRNA are aberrantly expressed in several cancers, including HNSCC.^(12–14) These studies suggest new approaches to the analysis of networks regulating cancer.

We have used miRNA expression signatures to identify anti-tumor miRNA that modulate novel cancer networks in HNSCC cells.^(15–18) More recently, we have analyzed miRNA signatures of HNSCC constructed by RNA-sequencing methods.⁽¹⁹⁾ These techniques are superior analytical methods for study of the transcriptome, and this strategy is leading to the discovery of novel dysregulated miRNA in cancer cells. Our signature showed that several miRNA passenger strands are aberrantly expressed in HNSCC.⁽¹⁹⁾ In miRNA biogenesis, it is believed that the passenger strand of miRNA is degraded and not incorporated into the RNA-induced silencing complex (RISC) and has no functional role in cells.^(10,20,21)

Our studies of miRNA signatures in HNSCC using RNA sequencing revealed that the *miR-199* family (*miR-199a-5p*, *miR-199a-3p*, *miR-199b-5p* and *miR-199b-3p*) was significantly reduced in cancer tissues. We hypothesized that both strands of pre-*miR-199a* (*miR-199a-5p* and *miR-199a-3p*) and pre-*miR-199b* (*miR-199b-5p* and *miR-199b-3p*) functioned as

anti-tumor miRNA targeting novel pathways. The aim of the present study was to investigate the functional significance of the *miR-199* family and the coordinately regulated oncogenic targets and pathways involved in HNSCC pathogenesis. Elucidation of antitumor molecular networks modulated by the *miR-199* family in HNSCC cells may provide new insight into the mechanisms of the disease.

Materials and Methods

Clinical head and neck squamous cell carcinoma specimens, cell lines and RNA extraction. A total of 22 clinical tissue specimens were collected from patients with HNSCC who underwent surgical resection at Chiba University Hospital between 2008 and 2013. The patients' backgrounds and clinicopathological characteristics are summarized in Table 1. All patients in this study provided informed consent and the study protocol was approved by the Institutional Review Board of Chiba University.

Two human HNSCC cell lines, SAS and HSC3, were investigated in this study. Both cell lines were obtained from RIKEN Cell Bank (Tsukuba, Ibaraki, Japan).

Total RNA, including miRNA, was isolated using TRIzol reagent (Invitrogen, Carlsbad, CA, USA) according to the manufacturer's protocol.

Quantitative real-time PCR. PCR quantification was carried out essentially as previously described.^(15,16,22) To quantify the expression level of miRNA, we utilized stem-loop quantitative RT-PCR (qRT-PCR) for *miR-199a-5p* (assay ID: 000498; Applied Biosystems, Foster City, CA, USA), *miR-199b-5p* (assay ID: 000500, Applied Biosystems) and *miR-199-3p* (assay ID: 002304, Applied Biosystems) following the manufacturer's protocol. TaqMan probes and primers for *Pri-miR-199a-1* (Hs03302808_pri, Applied Biosystems), *Pri-miR-199a-2* (Hs03302922_pri, Applied Biosystems), *Pri-miR-199b*

(Hs04227284_pri, Applied Biosystems) and *ITGA3* (Hs01076873_m1, Applied Biosystems) were assay-on-demand gene expression products. mRNA and miRNA data were normalized to human *GUSB* (assay ID: Hs99999908_m1; Applied Biosystems) and *RNU48* (assay ID: 001006; Applied Biosystems), respectively. The fold change was calculated using the delta-delta Ct method.

Preparation of a high purity fraction of miRNA based on an immunoprecipitation method. We investigated whether the passenger strand of miRNA was incorporated into RNA-induced silencing complex (RISC). We used a miRNA Isolation Kit, Human Ago2 (Wako, Osaka, Japan) to prepare a high purity fraction of microRNA based on an immunoprecipitation method using a high affinity anti-human Ago2 monoclonal antibody. The procedure was carried out according to the manufacturer's protocol.

Transfection of miRNA mimic, siRNA and plasmid vector into head and neck squamous cell carcinoma cell lines. Head and neck squamous cell carcinoma cell lines were transfected with miRNA mimics for gain-of-function experiments and siRNA for loss-of-function experiments. Pre-miR miRNA Precursors (*miR-199a-5p*; P/N: PM10893, *miR-199b-5p*; P/N: PM10553, *miR-199-3p*; P/N: PM11779 and negative control miR; P/N: AM17111; Applied Biosystems) were used. The following siRNA were used: stealth select RNAi siRNA, *si-ITGA3* (P/N: HSS105531 and HSS179967; Invitrogen). For transfection, RNA were incubated with OPTIMEM (Invitrogen) and Lipofectamine RNAiMAX Reagent (Invitrogen) as in previous studies.^(15,16,22) Plasmid vectors were incubated with OptiMEM and Lipofectamine 3000 reagent (Invitrogen) by forward transfection following the manufacturer's protocol.⁽²³⁾

Cell proliferation, migration and invasion assays. SAS and HSC3 cells were transfected with 10 nM miRNA or siRNA by reverse transfection. Cell proliferation, migration and invasion assays were carried out as previously described.^(15,16,22)

Identification of genes putatively regulated by *miR-199a-5p*, *miR-199b-5p* and *miR-199a/b-3p* in head and neck squamous cell carcinoma cells. Genes specifically affected by *miR-199-5p* and *miR-199a/b-3p* were identified by a combination of *in silico* and genome-wide gene expression analyses. Genes regulated by *miR-199-5p* and *miR-199a/b-3p* were listed using the TargetScan database (release 7.1). Genes upregulated in HNSCC were obtained from publicly available datasets in GEO (<http://www.ncbi.nlm.nih.gov/geo/>; accession number GSE9638). Our *in silico* analysis strategy behind this analysis procedure was described previously.^(15,16,22)

Plasmid construction and dual-luciferase reporter assays. The wide-type or deletion-type sequences of the 3'-untranslated region (UTR) of *ITGA3* in *miR-199a-5p*, *miR-199a/b-3p* and *miR-199b-5p* target sites were inserted in the psiCHECK-2 vector (C8021; Promega, Madison, WI, USA). The vectors were provided by Dr H. Yoshino from Kagoshima University.⁽²⁴⁾ The procedure for dual luciferase reporter assays was described previously.^(16,22)

Western blotting. Immunoblotting was performed with rabbit anti-ITGA3 antibody (1:250, HPA008572; SIGMA-ALDRICH, St. Louis, MO, USA), anti-Akt antibody (1:1000, #4691; Cell Signaling Technology, Danvers, MA, USA), anti-p-Akt antibody (1:1000, #4060; Cell Signaling Technology), anti-Erk1/2 antibody (1:1000, #4695; Cell Signaling Technology) and anti-p-Erk1/2 antibody (1:2000, #4370; Cell Signaling Technology), anti-FAK antibody (1:1000, #3285; Cell Signaling Technology) and anti-p-FAK antibody (1:1000, #8556; Cell Signaling Technology). Anti-GAPDH antibodies (1:1000, ab8245;

Table 1. Clinical features of 22 patients with head and neck squamous cell carcinoma

Number	Age	Sex	Location	T	N	M	Stage	Differentiation
1	64	F	Oral floor	4a	2c	0	IVA	Moderate
2	73	M	Tongue	3	2b	0	IVA	Poor
3	77	M	Tongue	2	2b	0	IVA	Poorly
4	63	F	Oral floor	2	2b	0	IVA	Basaloid SCC
5	59	M	Tongue	1	2a	0	IVA	Moderate
6	36	F	Tongue	3	1	0	III	Moderate
7	67	M	Tongue	3	0	0	III	Moderate
8	60	F	Tongue	2	1	0	III	Well
9	66	M	Tongue	2	0	0	II	Moderate
10	67	M	Tongue	2	0	0	II	Poor-moderate
11	76	F	Tongue	1	0	0	I	Well
12	69	M	Tongue	1	0	0	I	Well
13	73	F	Tongue	1	0	0	I	Well
14	64	M	Tongue	1	0	0	I	Well
15	70	M	Tongue	1	0	0	I	Well
16	38	M	Tongue	1	0	0	I	Well
17	51	M	Tongue	1	0	0	I	Well
18	34	F	Tongue	1	0	0	I	Poor
19	70	M	Tongue	1	0	0	I	Moderate
20	71	M	Tongue	1	0	0	I	Well
21	82	M	Oral floor	1	0	0	I	Well
22	81	M	Tongue	1	0	0	I	Extremely well

Abcam, Cambridge, UK) were used as an internal control. The procedures were performed as described in our previous studies.^(15,16,22)

The Cancer Genome Atlas database analysis of head and neck squamous cell carcinoma specimens. Head and neck squamous cell carcinoma specimens in the TCGA database (<https://tcga-data.nci.nih.gov/tcga/>) were divided into two groups (i.e. high and low expression of *ITGA3*). The groups were analyzed by Kaplan–Meier survival curves and log-rank statistics by using OncoLnc (<http://www.oncolnc.org>).⁽²⁵⁾ The genomic and clinical data were retrieved from cBioportal (<http://www.cbioportal.org/>), which were downloaded on 9 May 2017. Detailed information on the method is described in a previous paper.⁽²⁶⁾

Statistical analysis. The statistical analysis was undertaken as described in previous studies.^(15,16,19,22) All analyses were performed using Expert StatView (version 4; SAS Institute, Cary, NC, USA).

Results

Expression levels of *miR-199a-1*, *miR-199a-2* and *miR-199b* in head and neck squamous cell carcinoma clinical specimens and cell lines. We evaluated expression levels of *miR-199a-1*, *miR-*

199a-2 and *miR-199b* in HNSCC tissues ($n = 22$), normal epithelial tissues ($n = 22$) and two HNSCC cell lines (SAS and HSC3). Patient backgrounds and clinicopathological characteristics are summarized in Table 1. The stem-loop sequences of *miR-199a-1*, *miR-199a-2* and *miR-199b* are described in Figure 1a.

The expression levels of *miR-199a-1*, *miR-199a-2* and *miR-199b* were significantly lower in tumor tissues and HNSCC cell lines compared with normal epithelial tissues ($P = 0.0089$, $P = 0.0012$ and $P = 0.0029$, respectively; Fig. 1c).

Expression levels of *miR-199a-5p*, *miR-199b-5p* and *miR-199a/b-3p* in head and neck squamous cell carcinoma clinical specimens and cell lines. We evaluated expression levels of *miR-199a/b-5p* and *miR-199a/b-3p* in HNSCC tissues ($n = 22$), normal epithelial tissues ($n = 22$) and two HNSCC cell lines (SAS and HSC3). The *miR-199a-5p* sequence differs from the *miR-199b-5p* sequence by two nucleotides, and *miR-199a-3p* and *miR-199b-3p* have the same sequence (Fig. 1b).

The expression levels of *miR-199a-5p*, *miR-199b-5p* and *miR-199a/b-3p* were significantly lower in tumor tissues and HNSCC cell lines compared with normal epithelial tissues ($P = 0.0062$, $P < 0.0001$ and $P < 0.0001$, respectively; Fig. 1d).

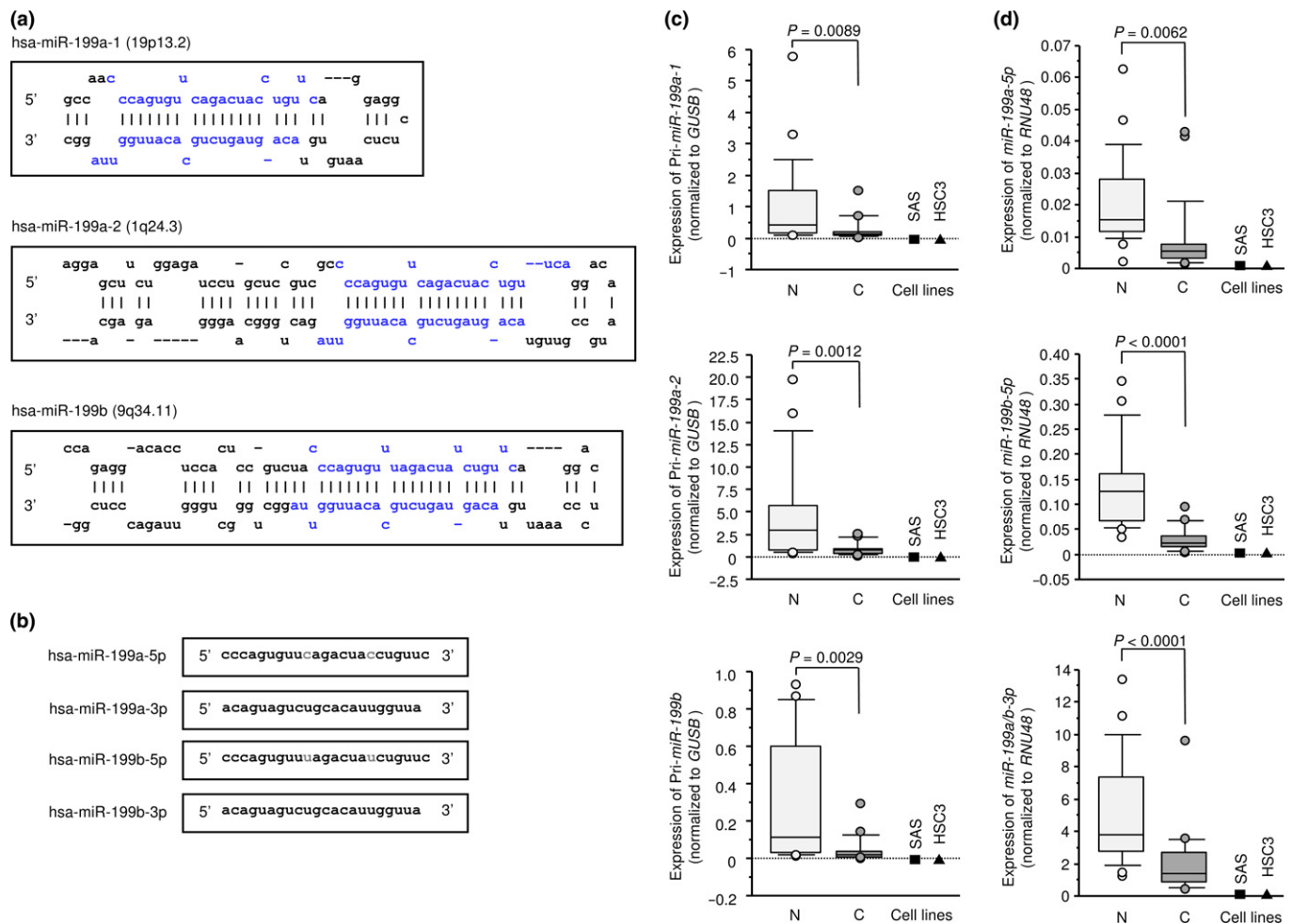


Fig. 1. Sequences of the *miR-199* family and expression levels of *miR-199* in head and neck squamous cell carcinoma (HNSCC) clinical specimens. (a) Stem-loop sequence of *miR-199a-1*, *miR-199a-2* and *miR-199b*, with blue characters indicating mature miRNA. (b) Mature miRNA sequences of the *miR-199* family, with red characters indicating variant nucleotides. (c) Expression levels of pri-*miR-199a-1*, pri-*miR-199a-2* and pri-*miR-199b* in HNSCC clinical specimens and cell lines. *GUSB* was used as an internal control. (d) Expression levels of *miR-199a-5p*, *miR-199b-5p* and *miR-199a/b-3p* in HNSCC clinical specimens and cell lines. *RNU48* was used as an internal control. C, cancer; N, normal tissue.

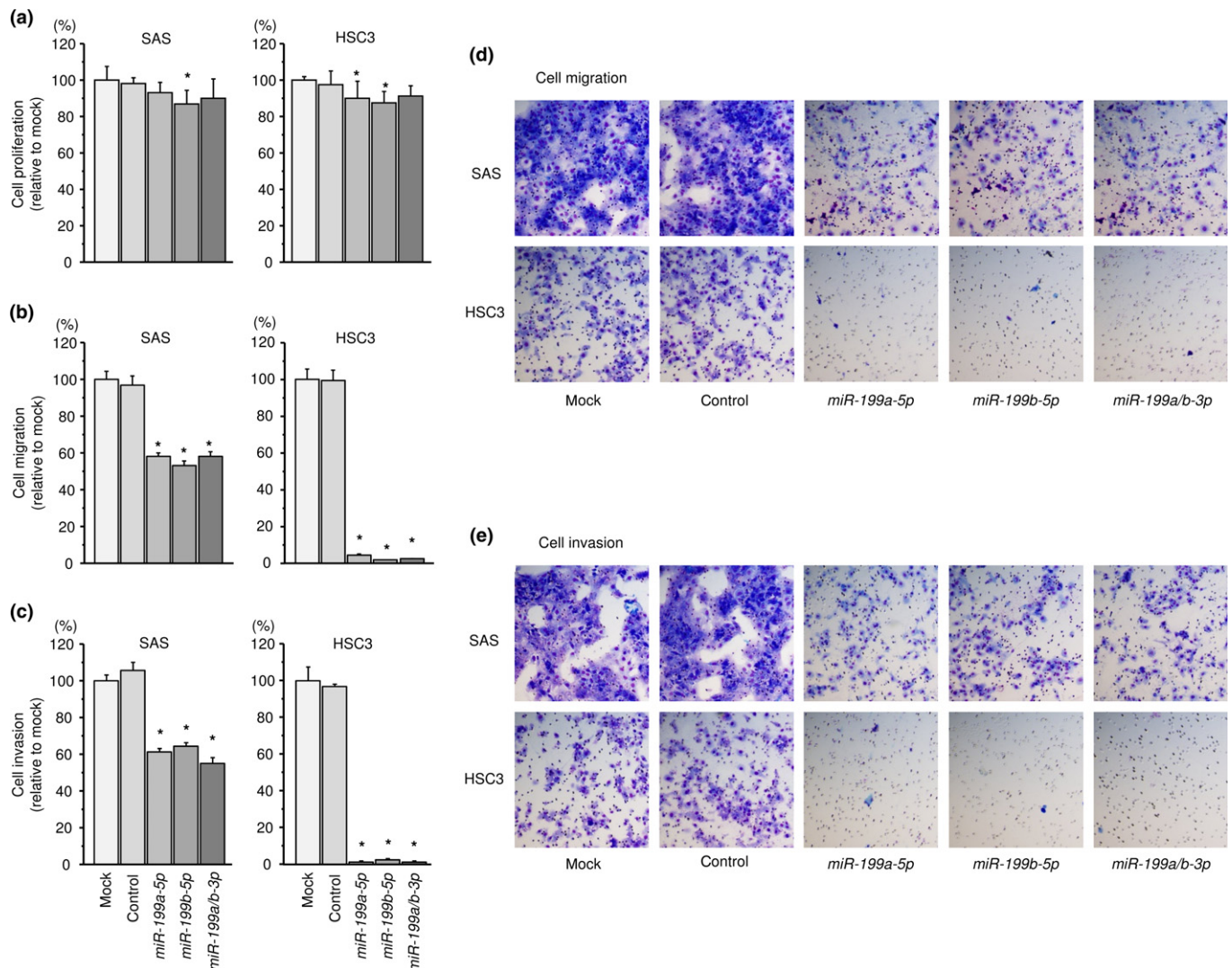


Fig. 2. Functional significance of *miR-199a/b-5p/3p* in head and neck squamous cell carcinoma (HNSCC) cells. (a) Cell proliferation was determined by XTT assay 72 h after transfection with *miR-199a-5p*, *miR-199b-5p* or *miR-199a/b-3p*. * $P < 0.05$. (b) Cell movement was assessed by migration assays 48 h after transfection with *miR-199a-5p*, *miR-199b-5p* or *miR-199a/b-3p*. * $P < 0.0001$. (c) Characterization of cell invasive capacity 48 h after transfection with *miR-199a-5p*, *miR-199b-5p* or *miR-199a/b-3p*. * $P < 0.0001$. (d) Phase micrographs of SAS and HSC3 cell lines in migration assays. (e) Phase micrographs of SAS and HSC3 cell lines in invasion assays (100 × magnification field).

Effects of *miR-199a-5p*, *miR-199b-5p* and *miR-199a/b-3p* expression on cell proliferation, migration and invasion in head and neck squamous cell carcinoma cell lines. XTT assays demonstrated that proliferation was not inhibited in *miR-199a-5p*, *miR-199b-5p* or *miR-199a/b-3p* transfectants in comparison with mock in SAS and HSC3 cells (Fig. 2a). In contrast, there was significant inhibition of cell migration activity after transfection with *miR-199a-5p*, *miR-199b-5p* or *miR-199a/b-3p* (* $P < 0.0001$; Fig. 2b). Phase micrographs of SAS and HSC3 cell lines in migration assays are shown in Figure 2d. Similarly, Matrigel invasion assays revealed that transfection with *miR-199a-5p*, *miR-199b-5p* or *miR-199a/b-3p* reduced cell invasion activities (* $P < 0.0001$; Fig. 2c). Phase micrographs of SAS and HSC3 cell lines in invasion assays are shown in Figure 2e.

Incorporation of the *miR-199* family into RISC in SAS cells. To confirm that *miR-199* family members were actually functioning in cells, we used RT-PCR to demonstrate that restored mature miRNA was incorporated into the RISC. The schema of this

procedure is shown in Figure 3a. Expression of *miR-199a-5p* was significantly higher than that in cells transfected with mock, miR control, *miR-199b-5p* or *miR-199a/b-3p* ($P < 0.0001$; Fig. 3b). Likewise, expression of *miR-199b-5p* was significantly higher than that in cells transfected with mock, miR control, *miR-199a-5p* or *miR-199a/b-3p* ($P < 0.0001$; Fig. 3b). Expression of *miR-199a/b-3p* was significantly higher than that in cells transfected with mock or miR control, *miR-199a-5p* or *miR-199b-5p* ($P < 0.0001$; Figure 3b).

Identification of target genes coordinately regulated by the *miR-199* family in head and neck squamous cell carcinoma cells. To identify target genes coordinately regulated by *miR-199-5p* and *miR-199-3p*, we combined several *in silico* analyses. Our strategy for selection of those genes is shown in Figure 4.

The TargetScan database (release 7.1) showed that 621 and 469 genes have putative target sites for *miR-199-5p* and *miR-199-3p*, respectively, in their 3'-UTR. First, to evaluate upregulated genes in clinical HNSCC specimens, we examined gene expression profiles in the GEO database (accession number

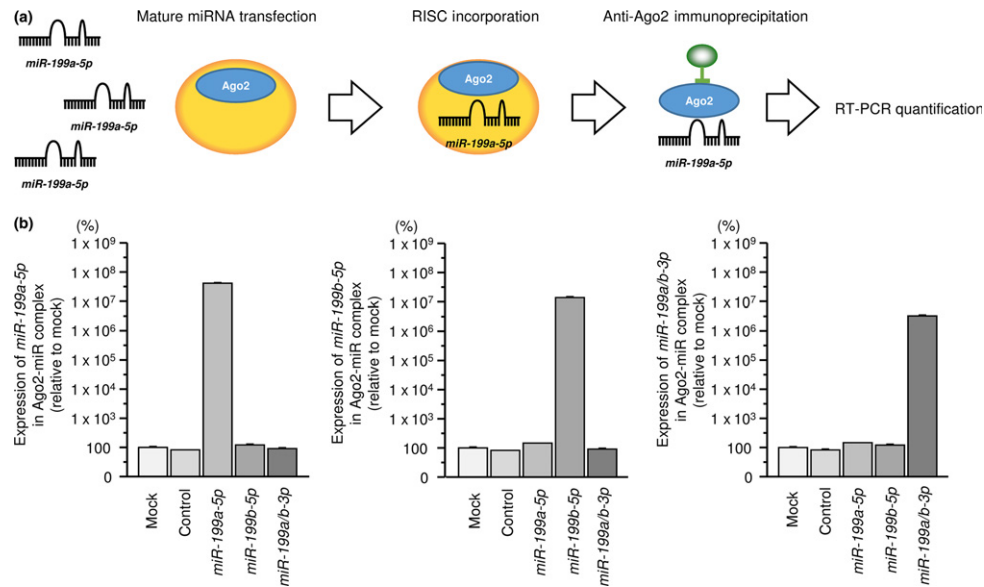


Fig. 3. Incorporation of the *miR-199* family into the RNA-induced silencing complex (RISC) in SAS cells. (a) Mature microRNA was transfected into SAS cells, and it was incorporated into the RISC. The incorporated microRNA was prepared to high purity using immunoprecipitation with anti-human Ago2 monoclonal antibody. Expression of the microRNA was quantified with RT-PCR. (b) Expression of *miR-199a-5p* was significantly higher than that in cells transfected with mock, miR control, *miR-199b-5p* or *miR-199a/b-3p* ($P < 0.0001$). Likewise, expression of *miR-199b-5p* was significantly higher than that in cells transfected with mock, miR control, *miR-199a-5p* or *miR-199a/b-3p* ($P < 0.0001$). Expression of *miR-199a/b-3p* was significantly higher than that in cells transfected with mock, miR control, *miR-199a-5p* or *miR-199b-5p* ($P < 0.0001$).

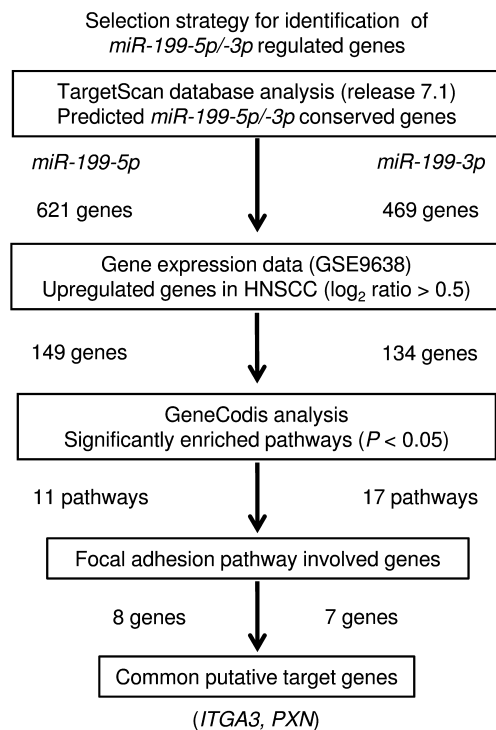


Fig. 4. Flow chart depicting the strategy for identification of *miR-199-5p* and *miR-199-3p* target genes. Analysis using the TargetScan database showed that 621 and 469 genes had putative target sites for *miR-199-5p/3p*, respectively, in their 3'-UTR. Then, we assessed the expression levels of those genes using the GEO database (GSE9638). Finally, we categorized these putative target genes into KEGG pathways using the GeneCodis database, and 11 and 17 pathways were identified. Among these pathways, we focused on the "focal adhesion pathway" because *miR-199-5p/3p* markedly inhibited cancer cell migration and invasion. The data showed that two genes (*ITGA3* and *PXN*) were regulated by both *miR-199-5p/3p*.

Table 2. Significantly enriched annotations regulated by *miR-199-5p*

Number of genes	P-value	Annotations
8	9.2E-05	(KEGG) 04510: Focal adhesion
5	1.0E-04	(KEGG) 05217: Basal cell carcinoma
10	1.2E-04	(KEGG) 05200: Pathways in cancer
6	9.2E-04	(KEGG) 04310: Wnt signaling pathway
4	1.6E-03	(KEGG) 04340: Hedgehog signaling pathway
6	3.9E-03	(KEGG) 04810: Regulation of actin cytoskeleton
4	4.7E-03	(KEGG) 05222: Small cell lung cancer
4	4.7E-03	(KEGG) 04512: ECM-receptor interaction
4	6.7E-03	(KEGG) 04916: Melanogenesis
3	6.8E-03	(KEGG) 02010: ABC transporters
3	2.8E-02	(KEGG) 05412: Arrhythmogenic right ventricular cardiomyopathy

GSE9638). A total of 149 and 134 genes were identified as putative target genes for *miR-199-5p* and *miR-199-3p*, respectively, in HNSCC cells.

Next, we categorized these putative target genes by reference to the Kyoto Encyclopedia of Genes and Genomes (KEGG) pathways using the GeneCodis database, and 11 and 17 pathways were identified as significantly enriched pathways (Tables 2 and 3). Among these, we focused on the "focal adhesion pathway" because *miR-199-5p* and *miR-199-3p* markedly inhibited cancer cell migration and invasion (Fig. 2b,c). Two genes (*ITGA3* and *PXN*) were regulated by both *miR-199-5p* and *miR-199-3p* (Tables 4 and 5). We focused on *ITGA3* because according to our previous studies, aberrant integrin-mediated signaling promoted cancer cell aggressiveness.^(23,27,28)

***miR-199-5p* and *miR-199-3p* controlled the expression of *ITGA3* in head and neck squamous cell carcinoma cells.** We assessed the Kaplan–Meier univariate survival of patient groups using a

Table 3. Significantly enriched annotations regulated by *miR-199-3p*

Number of genes	P-value	Annotations
7	3.8E-06	(KEGG) 04512: ECM-receptor interaction
8	8.0E-05	(KEGG) 04810: Regulation of actin cytoskeleton
7	3.9E-04	(KEGG) 04510: Focal adhesion
5	6.1E-04	(KEGG) 05414: Dilated cardiomyopathy
4	3.6E-03	(KEGG) 05412: Arrhythmogenic right ventricular cardiomyopathy
4	3.9E-03	(KEGG) 05222: Small cell lung cancer
4	4.0E-03	(KEGG) 05410: Hypertrophic cardiomyopathy (HCM)
7	4.5E-03	(KEGG) 05200: Pathways in cancer
4	7.1E-03	(KEGG) 05146: Amoebiasis
3	2.2E-02	(KEGG) 04971: Gastric acid secretion
3	2.2E-02	(KEGG) 05100: Bacterial invasion of epithelial cells
3	2.3E-02	(KEGG) 04730: Long-term depression
3	3.0E-02	(KEGG) 04970: Salivary secretion
3	3.0E-02	(KEGG) 04640: Hematopoietic cell lineage
3	3.1E-02	(KEGG) 04540: Gap junction
3	3.7E-02	(KEGG) 04912: GnRH signaling pathway
3	3.7E-02	(KEGG) 04972: Pancreatic secretion

TCGA database, comparing those with a high expression level of *ITGA3* and those with a low expression level of *ITGA3*. Figure 5a shows that the *ITGA3* high expression group had a significantly poorer overall survival rate ($P = 0.0048$). Moreover, high expression of *ITGA3* was associated with disease-free survival ($P = 0.0338$) (Fig. 5a). Multivariate Cox proportional hazards models were used to assess independent predictors of progression-free survival, including the expression level of the gene (Z score > 0 vs Z score ≤ 0), tumor stage (T3 and T4 vs T1 and T2), lymph node stage (N+ vs N-), age at diagnosis (>60 years vs ≤ 60 years), histologic

grade (G3 and G4 vs G1 and G2) and sex (male vs female). High *ITGA3* expression was a significant prognostic factor in patients with HNSCC (hazard ratio [HR] = 1.48, 95% confidence interval [CI] = 1.08–2.04, $P = 0.015$; Table 6).

We investigated the mRNA expression levels of *ITGA3* in 22 HNSCC clinical specimens by qRT-PCR. *ITGA3* was significantly upregulated in HNSCC tumor tissues ($P = 0.0005$; Fig. 5b). Spearman's rank test showed a negative correlation between the expression of *ITGA3* and *miR-199a-5p* ($P = 0.0055$, $R = -0.422$; Fig. 5c), the expression of *ITGA3* and *miR-199b-5p* ($P = 0.0004$, $R = -0.541$; Fig. 5c) and the expression of *ITGA3* and *miR-199a/b-3p* ($P = 0.0029$, $R = -0.454$; Fig. 5c).

***ITGA3* was directly regulated by *miR-199* family in head and neck squamous cell carcinoma cells.** We also investigated whether *ITGA3* expression was reduced by restoration of *miR-199a-5p*, *miR-199b-5p* and *miR-199a/b-3p* in HNSCC cells. The expression levels of *ITGA3* mRNA and protein were significantly repressed in *miR-199a-5p*, *miR-199b-5p* and *miR-199a/b-3p* transfectants compared with mock cells (Fig. 6a,b).

We performed dual-luciferase reporter assays in SAS cells to determine whether the *ITGA3* was directly regulated by *miR-199a-5p*, *miR-199a/b-3p* and *miR-199b-5p*. Seed sequences of *miR-199a-5p* and *miR-199b-5p* are identical. We used vectors encoding the partial wild-type or deletion-type sequences of the 3'-UTR of the *ITGA3* with *miR-199* family target sites. We detected that the luminescence intensities were significantly reduced by co-transfection with *miR-199a-5p*, *miR-199a/b-3p* and *miR-199b-5p* the vectors carrying the wild type (Fig. 6c). In contrast, transfection with the deletion-type vector blocked the reduction of luminescence intensities (Fig. 6c). These findings indicated that *miR-199* family directly bound specific sites in the 3'-UTR of *ITGA3*.

Effects of *ITGA3* knockdown on cell proliferation, migration and invasion in head and neck squamous cell carcinoma cells. First, we evaluated the knockdown efficiency of *si-ITGA3* transfection in SAS and HSC3 cell lines. qRT-PCR data and

Table 4. Focal adhesion pathway regulated by *miR-199-5p*

Gene symbol	Gene name	Conserved	Poorly conserved	GEO9638 log ₂ ratio
COL5A3	Collagen, type V, alpha 3	1	0	1.373
PPP1R12A	Protein phosphatase 1, regulatory (inhibitor) subunit 12A	1	0	0.797
PXN	Paxillin	1	0	0.774
LAMC1	Laminin, gamma 1 (formerly LAMB2)	1	0	0.657
VEGFA	Vascular endothelial growth factor A	1	0	0.653
ITGA4	Integrin, alpha 4 (antigen CD49D, alpha 4 subunit of VLA-4 receptor)	1	0	0.618
GSK3B	Glycogen synthase kinase 3 beta	2	0	0.606
ITGA3	Integrin, alpha 3 (antigen CD49C, alpha 3 subunit of VLA-3 receptor)	1	3	0.583

Table 5. Focal adhesion pathway regulated by *miR-199-3p*

Gene symbol	Gene name	Conserved	Poorly conserved	GEO9638 log ₂ ratio
FN1	Fibronectin 1	1	1	1.831
COL4A5	Collagen, type IV, alpha 5	1	1	1.364
ITGA1	Integrin, alpha 1	3	2	1.249
ITGA6	Integrin, alpha 6	1	0	1.105
PXN	Paxillin	1	0	0.774
ITGB8	Integrin, beta 8	2	0	0.697
ITGA3	Integrin, alpha 3 (antigen CD49C, alpha 3 subunit of VLA-3 receptor)	1	0	0.583

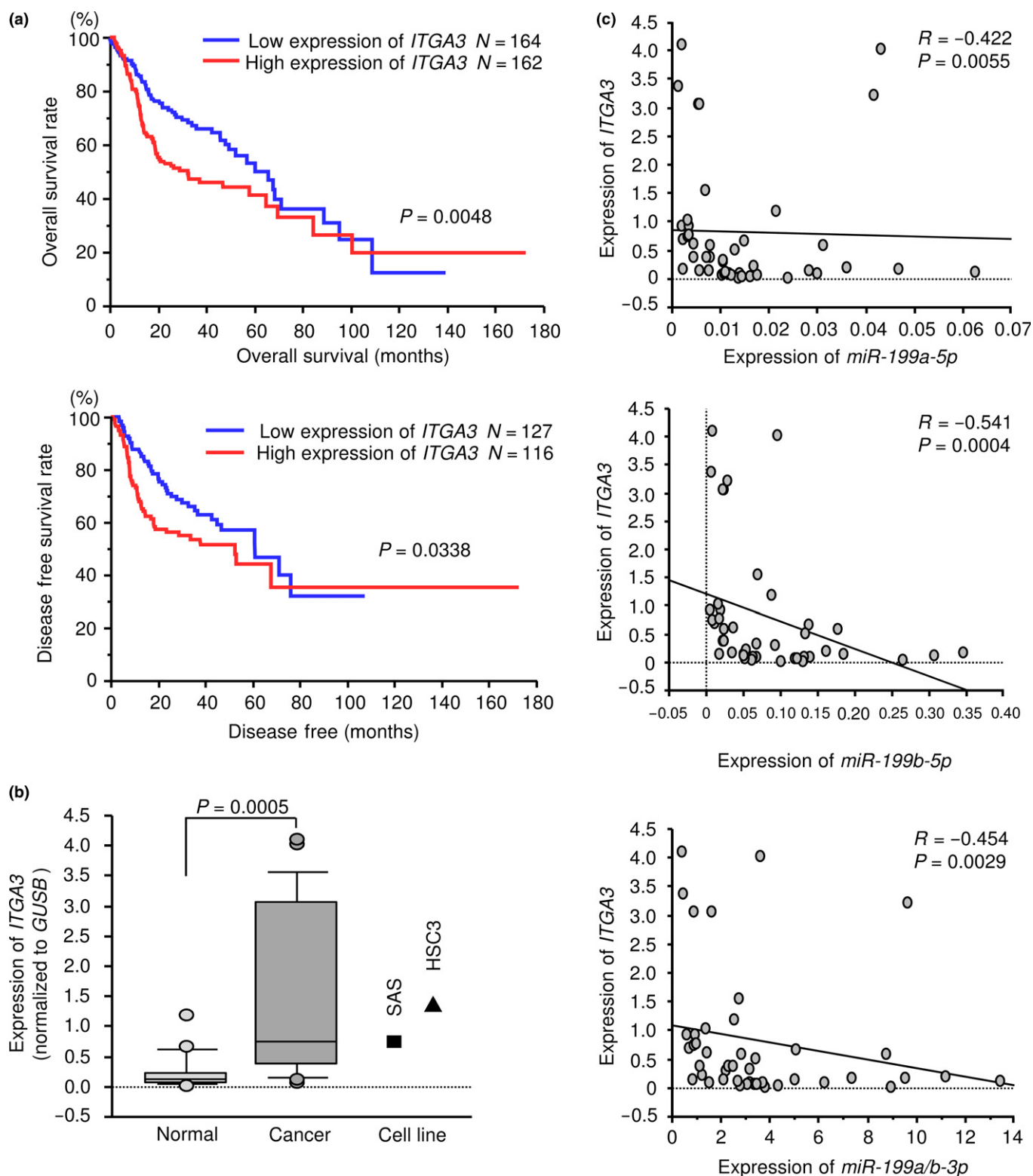


Fig. 5. Regulation of target gene expression by *miR-199-5p* and *miR-199-3p* in head and neck squamous cell carcinoma (HNSCC) clinical specimens and HNSCC cell lines. (a) Kaplan-Meier survival curves, as determined using data from the TCGA database. (b) Expression levels of *ITGA3* in HNSCC clinical specimens and cell lines. *GUSB* was used as an internal control. (c) The negative correlations between *ITGA3* expression and the expression of *miR-199a/b-5p/3p*. Spearman's rank test was used to evaluate the correlation.

western blotting indicated that the siRNA effectively downregulated *ITGA3* expression (Fig. 7a,b).

XTT assays demonstrated that SAS and HSC3 cell proliferation was not inhibited by *si-ITGA3* transfection compared with

mock (Fig. 7c). In contrast, migration of SAS and HSC3 cell lines was significantly inhibited in *si-ITGA3* transfectants in comparison with mock (Fig. 7d). We also found that the invasion activities of SAS and HSC3 cells were significantly

Table 6. Hazard ratio and 95% CI of each subgroup in TCGA database

Factor	HR	95% CI	P-value
<i>ITGA3</i> expression ($Z > 0$ vs $Z \leq 0$)	1.48	1.08–2.04	0.015
T stage (T3&4 vs T1&2)	2.06	1.42–3.09	<0.0001
N stage (N+ vs N-)	1.92	1.37–2.73	<0.0001
Histologic grade (G3&4 vs G1&2)	0.95	0.66–1.35	0.796
Age (>60 vs ≤60)	1.19	0.86–1.65	0.295
Gender (male vs female)	0.78	0.55–1.11	0.162

inhibited after *si-ITGA3* transfection in comparison with mock transfection (Fig. 7e).

Effects of co-transfection of *ITGA3/miR-199s* in SAS cells. To validate whether the *ITGA3/miR-199* family axis was critical for the progression of HNSCC, we performed *ITGA3* rescue experiments by co-transfection with *ITGA3* and the *miR-199* family in SAS cells (Fig. S1). The results showed that the migration and invasion abilities of SAS cells were recovered by *ITGA3* and *miR-199* family transfection compared with cells that restored each *miR-199* family only (Fig. 8). These

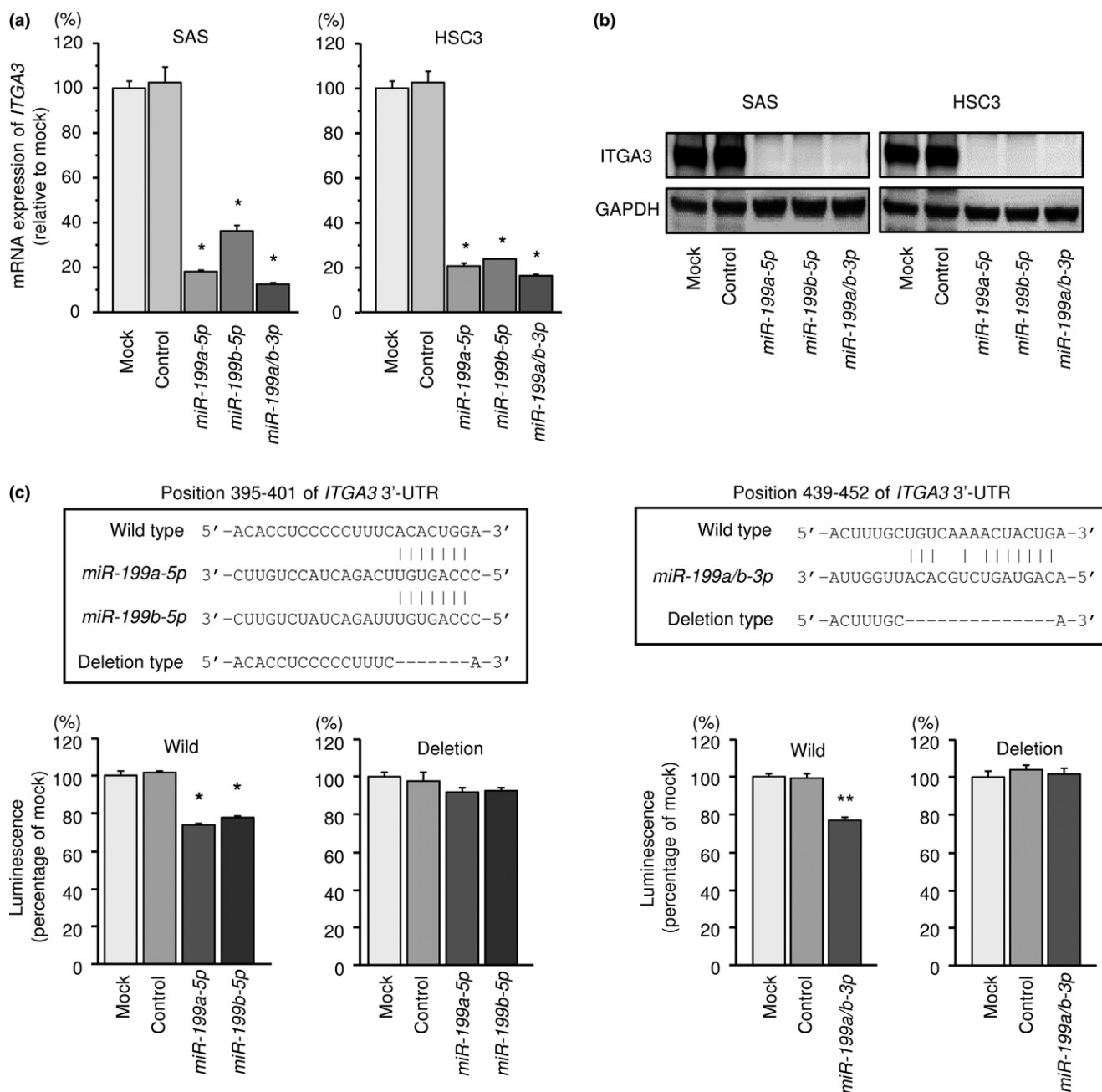


Fig. 6. Direct regulation of *ITGA3* by *miR-199* family in head and neck squamous cell carcinoma (HNSCC) cells. (a) Expression levels of *ITGA3* mRNA 72 h after transfection with 10 nM *miR-199a-5p*, *miR-199b-5p* or *miR-199a/b-3p* into cell lines. *GUSB* was used as an internal control. * $P < 0.0001$. (b) Protein expression of *ITGA3* 72 h after transfection with *miR-199a-5p*, *miR-199b-5p* or *miR-199a/b-3p*. GAPDH was used as a loading control. (c) *miR-199* family binding sites in the 3'-UTR of *ITGA3* mRNA. Dual luciferase reporter assays using vectors encoding putative *miR-199* family target sites of the *ITGA3* 3' UTR (positions 395–401 and 439–452) for wild type and deletion type. Normalized data were calculated as ratios of *Renilla*/firefly luciferase activities. * $P < 0.0001$, ** $P < 0.05$.

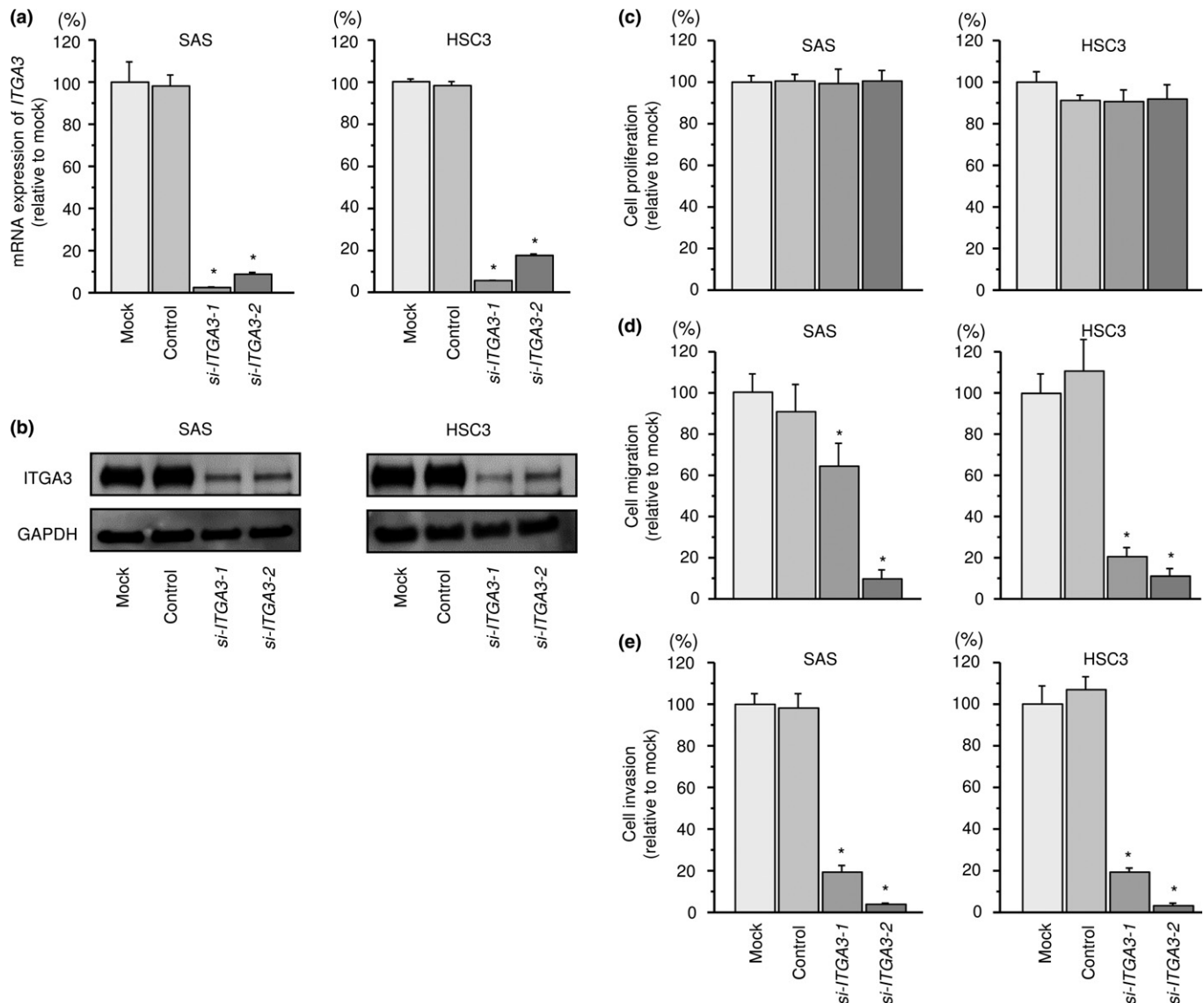


Fig. 7. Effects of *ITGA3* silencing by siRNA transfection in head and neck squamous cell carcinoma (HNSCC) cells. (a) *ITGA3* mRNA expression 72 h after transfection of 10 nM siRNA into HNSCC cells. *GUSB* was used as an internal control. * $P < 0.0001$. (b) *ITGA3* protein expression 72 h after transfection with siRNA. GAPDH was used as a loading control. (c) Cell proliferation was determined by XTT assay 72 h after transfection with siRNA. (d) Cell movement was assessed by migration assay 48 h after transfection with siRNA. * $P < 0.0001$. (e) Characterization of invasion 48 h after transfection with siRNA. * $P < 0.0001$.

findings suggested that *ITGA3* was involved in cancer cell migration and invasion in HNSCC cells.

Effects of *ITGA3* knockdown on downstream signaling. We analyzed the effects of downstream oncogenic signaling of *ITGA3* by using siRNA transfection of SAS cells. The phosphorylation status of AKT (Ser 473), ERK1/2 (Thr 202/Tyr 204) and FAK (Tyr 397) was examined. Knockdown of *ITGA3* reduced the phosphorylation of AKT, ERK1/2 and FAK in SAS cells (Fig. 9).

We also investigated whether the expression of *miR-199* family (*miR-199a-5p*, *miR-199a/b-3p* and *miR-199b-5p*) affected downstream signaling. Restoration of *miR-199* family reduced phosphorylation of AKT, ERK1/2 and FAK in SAS cells (Fig. 9).

Discussion

New therapeutic strategies are needed to improve the poor prognosis of HNSCC patients with metastasis. To achieve that

goal, novel regulatory networks that promote HNSCC cellular metastasis must be identified and targeted. Towards that end, we have identified anti-tumor miRNA-modulated pathways that promote the aggressive behavior of various cancer cells, including HNSCC cells.^(15–18,22,29–34) Our past studies showed that anti-tumor miRNA, including *miR-26a/b*, *miR-29a/b/c* and *miR-218*, concertedly regulated the lysyl oxidase-like 2 (*LOXL2*) gene in cancer cells.^(29–34) The basic function of *LOXL2* is covalent crosslinking of collagen and/or elastin in the extracellular matrix (ECM).⁽³⁵⁾ Overexpression of *LOXL2* was correlated with disease progression of several cancers and induced the epithelial–mesenchymal transition (EMT) by interaction with transcription factor *SNAIL1*.⁽³⁶⁾ Our miRNA-based strategy can efficiently identify novel molecular pathways involved in cancer pathogenesis.

More recently, we have analysed the miRNA signature of HNSCC clinical specimens by using RNA-sequencing

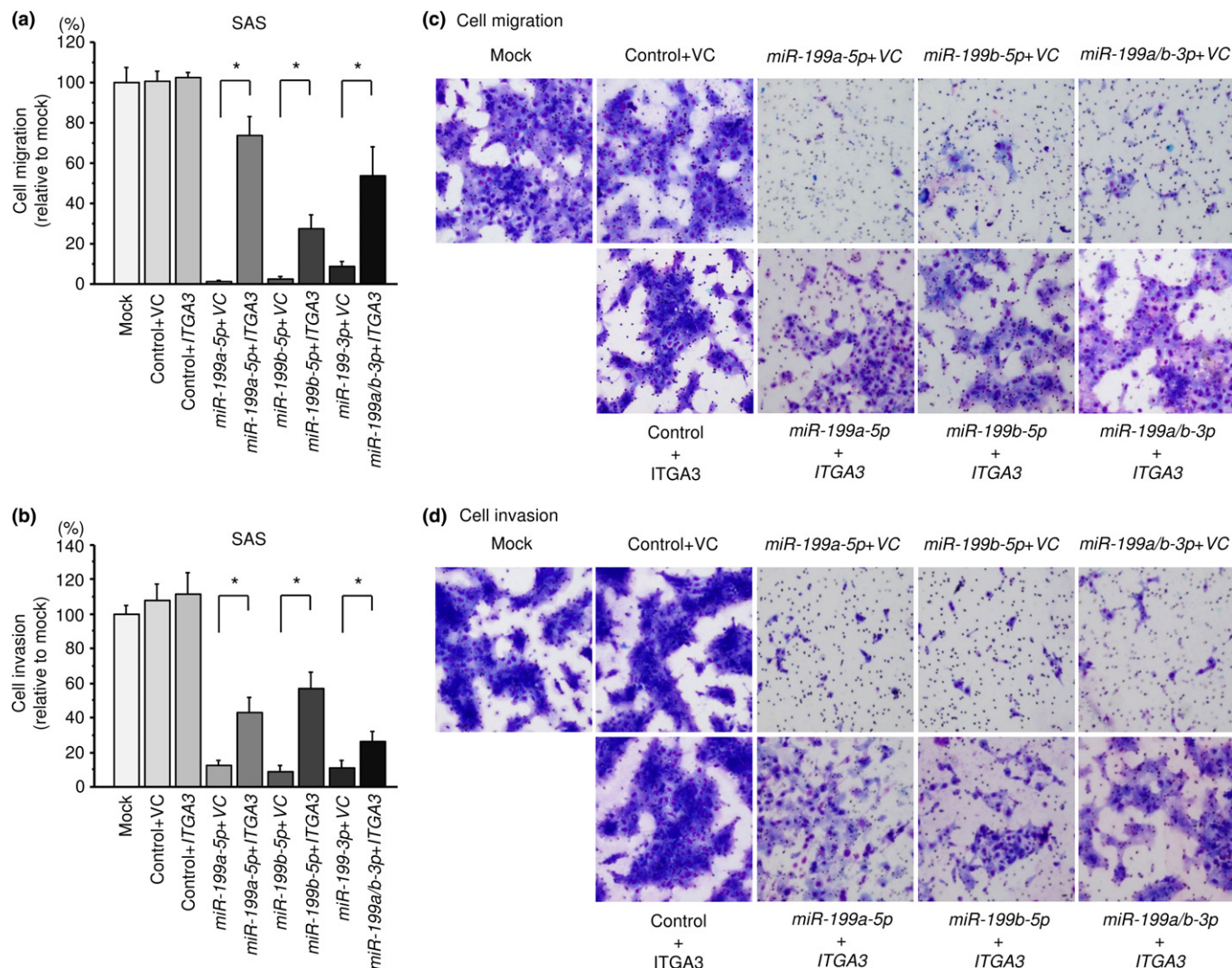


Fig. 8. Effects of co-transfection of *ITGA3/miR-199* family in SAS cells. (a) Cell migration activity was assessed by wound-healing assays 48 h after reverse transfection with *miR-199* family and 24 h after forward transfection with the *ITGA3* vector. * $P < 0.0001$. (b) Cell invasion activity was characterized by invasion assays 48 h after reverse transfection with *miR-199* family and 48 h after forward transfection with *ITGA3* vector. * $P < 0.0001$. (c,d) Phase micrographs of SAS cell line in migration and invasion assays (100 × magnification field).

technology.⁽¹⁹⁾ Our signature revealed that several passenger strands of miRNA, such as *miR-143-3p*, *miR-145-3p* and *miR-150-3p*, were downregulated in HNSCC tissues.⁽¹⁹⁾ In general, passenger strands of miRNA are degraded without incorporation into the RISC.^(10,20,21) In contrast, our signatures indicate that some passenger strands of miRNA function in cancer cells. We recently showed that passenger strands of certain miRNA (*miR-144-5p*, *miR-145-3p* and *miR-139-3p*) acted as anti-tumor miRNA through their targeting of several oncogenic genes.^(37–40) Our results have changed the concept of miRNA biogenesis and the role of passenger strands, opening up new approaches in miRNA research.

In this study, we focused on the *miR-199* family (*miR-199a-5p*, *miR-199a-3p*, *miR-199b-5p* and *miR-199b-3p*) because all members of the family were significantly reduced in our RNA sequencing-based miRNA signature of HNSCC. We hypothesized that dual strands of pre-*miR-199a* and pre-*miR-199b* acted as anti-tumor miRNA and were involved in HNSCC pathogenesis. Our functional assays showed that ectopic expression of all members of the *miR-199* family inhibited

cancer cell aggressiveness, indicating that the family acted as anti-tumor miRNA in HNSCC cells. The anti-tumor function of *miR-199a-5p* was reported in several types of cancers.^(41–43) With regard to *miR-199a-5p*, recent data showed that *miR-199a-3p* was downregulated in osteosarcoma and that restoration of *miR-199a-3p* significantly inhibited CD44 expression.⁽⁴⁴⁾ In prostate cancer, *miR-199a-3p* contributed to tumorigenic cancer stem cells through its targeting of *CD44*, *c-MYC*, *CCND1* and *EGFR*.⁽⁴⁵⁾ Several studies suggested that downregulated *miR-199b-5p* was involved in progression and metastasis in several cancers.^(46,47) Our present data describing the antitumor functions of the *miR-199* family in HNSCC cells are consistent with past studies.

To elucidate the contributions of the *miR-199* family to HNSCC pathogenesis, we analyzed the molecular networks that it regulated. We identified 2 putative targets in HNSCC cells that were modulated by the *miR-199* family, *ITGA3* and *PXN*. Here, we focused on the *ITGA3* gene because our previous studies indicated that dysregulated ECM and integrin-mediated oncogenic signaling enhanced cancer cell migration

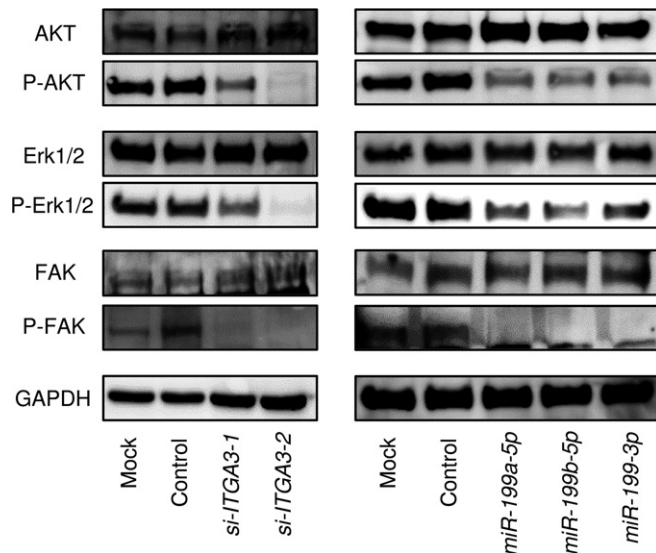


Fig. 9. Effects of the gene encoding ITGA3 protein on downstream signaling. (a) Knockdown of ITGA3 and (b) restoration of *miR-199* family in SAS cells reduced the phosphorylation of AKT, Erk1/2 and FAK. GAPDH was used as a loading control.

and invasion.⁽²³⁾ Our present data demonstrated that all members of the *miR-199* family regulated *ITGA3* in HNSCC cells. Moreover, knockdown of *ITGA3* inhibited cancer cell aggressiveness through regulating downstream oncogenic signaling.

References

- Leemans CR, Braakhuis BJ, Brakenhoff RH. The molecular biology of head and neck cancer. *Nat Rev Cancer* 2011; **11**: 9–22.
- Massano J, Regateiro FS, Janeiro G, Ferreira A. Oral squamous cell carcinoma: Review of prognostic and predictive factors. *Oral Surg Oral Med Oral Pathol Oral Radiol Endod* 2006; **102**: 67–76.
- Bhattacharya A, Roy R, Snijders AM *et al.* Two distinct routes to oral cancer differing in genome instability and risk for cervical node metastasis. *Clin Cancer Res* 2011; **17**: 7024–34.
- Wikner J, Grobe A, Pantel K, Riethdorf S. Squamous cell carcinoma of the oral cavity and circulating tumour cells. *World J Clin Oncol* 2014; **5**: 114–24.
- Siegel RL, Miller KD, Jemal A. Cancer statistics, 2016. *CA Cancer J Clin* 2016; **66**: 7–30.
- Bonner JA, Harari PM, Giralt J *et al.* Radiotherapy plus cetuximab for squamous-cell carcinoma of the head and neck. *N Engl J Med* 2006; **354**: 567–78.
- Bonner JA, Harari PM, Giralt J *et al.* Radiotherapy plus cetuximab for locoregionally advanced head and neck cancer: 5-year survival data from a phase 3 randomised trial, and relation between cetuximab-induced rash and survival. *Lancet Oncol* 2010; **11**: 21–8.
- Bartel DP. MicroRNAs: Genomics, biogenesis, mechanism, and function. *Cell* 2004; **116**: 281–97.
- Lewis BP, Burge CB, Bartel DP. Conserved seed pairing, often flanked by adenosines, indicates that thousands of human genes are microRNA targets. *Cell* 2005; **120**: 15–20.
- Bartel DP. MicroRNAs: Rarget recognition and regulatory functions. *Cell* 2009; **136**: 215–33.
- Iorio MV, Croce CM. MicroRNAs in cancer: Small molecules with a huge impact. *J Clin Oncol* 2009; **27**: 5848–56.
- Wiemer EA. The role of microRNAs in cancer: No small matter. *Eur J Cancer* 2007; **43**: 1529–44.
- Sethi N, Wright A, Wood H, Rabbitts P. MicroRNAs and head and neck cancer: Reviewing the first decade of research. *Eur J Cancer* 2014; **50**: 2619–35.
- Tran N, O'Brien CJ, Clark J, Rose B. Potential role of micro-RNAs in head and neck tumorigenesis. *Head Neck* 2010; **32**: 1099–111.

Integrin $\alpha\beta 1$ is abundant in human tissues and its aberrant expression has been implicated in the development and progression of cancer.^(23,48,49) Several studies demonstrated that overexpression of integrin $\alpha\beta 1$ contributed to cancer cell invasion. Moreover, overexpression was positively correlated with poor prognosis of the patients.⁽⁵⁰⁾

A large cohort study using data from the TCGA database indicated that high expression of *ITGA3* predicted poorer survival of HNSCC patients. Interestingly, Kaplan–Meier survival curves showed that high expression of *ITGB1* predicted poorer survival in patients with HNSCC. These findings indicate that overexpression of integrin $\alpha\beta 1$ could be deeply involved in HNSCC pathogenesis. Recent studies demonstrated that TGF- β stimulates the expression of integrin $\alpha\beta 1$ by transcriptional upregulation through the Ets transcription factor.⁽⁵¹⁾ Moreover, activation of $\alpha\beta 1$ -mediated signaling upregulated several oncogenic gene expression and enhanced metastatic phenotypes.^(50,52) Therefore, it is important to better understand integrin $\alpha\beta 1$ -mediated gene regulation in normal cells as well as in cancer cells.

Acknowledgments

This study was supported by JSPS KAKENHI, 16K20229, 15K10801, 25462676 and 26462596.

Disclosure Statement

The authors have no conflicts of interest to declare.

- Fukumoto I, Kinoshita T, Hanazawa T *et al.* Identification of tumour suppressive microRNA-451a in hypopharyngeal squamous cell carcinoma based on microRNA expression signature. *Br J Cancer* 2014; **111**: 386–94.
- Fukumoto I, Hanazawa T, Kinoshita T *et al.* MicroRNA expression signature of oral squamous cell carcinoma: Functional role of microRNA-26a/b in the modulation of novel cancer pathways. *Br J Cancer* 2015; **112**: 891–900.
- Kikkawa N, Hanazawa T, Fujimura L *et al.* miR-489 is a tumour-suppressive miRNA target PTPN11 in hypopharyngeal squamous cell carcinoma (HSCC). *Br J Cancer* 2010; **103**: 877–84.
- Nohata N, Hanazawa T, Kikkawa N *et al.* Tumour suppressive microRNA-874 regulates novel cancer networks in maxillary sinus squamous cell carcinoma. *Br J Cancer* 2011; **105**: 833–41.
- Koshizuka K, Nohata N, Hanazawa T *et al.* Deep sequencing-based microRNA expression signatures in head and neck squamous cell carcinoma: Dual strands of pre-miR-150 as antitumor miRNAs. *Oncotarget* 2017; **8**: 30288–304.
- Chendrimada TP, Gregory RI, Kumaraswamy E *et al.* TRBP recruits the Dicer complex to Ago2 for microRNA processing and gene silencing. *Nature* 2005; **436**: 740–4.
- Hutvagner G, Zamore PD. A microRNA in a multiple-turnover RNAi enzyme complex. *Science (New York, NY)* 2002; **297**: 2056–60.
- Koshizuka K, Hanazawa T, Fukumoto I *et al.* Dual-receptor (EGFR and c-MET) inhibition by tumor-suppressive miR-1 and miR-206 in head and neck squamous cell carcinoma. *J Hum Genet* 2017; **62**: 113–21.
- Kurozumi A, Goto Y, Matsushita R *et al.* Tumor-suppressive microRNA-223 inhibits cancer cell migration and invasion by targeting ITGA3/ITGB1 signaling in prostate cancer. *Cancer Sci* 2016; **107**: 84–94.
- Sakaguchi T, Yoshino H, Yonemori M *et al.* Regulation of ITGA3 by the dual-stranded microRNA-199 family as a potential prognostic marker in bladder cancer. *Br J Cancer* 2017; **116**: 1077–87.
- Anaya J. OncoLnc: linking TCGA survival data to mRNAs, miRNAs, and lncRNAs. *PeerJ CompSci* 2016; **2**: e67.
- Gao J, Aksoy BA, Dogrusoz U *et al.* Integrative analysis of complex cancer genomics and clinical profiles using the cBioPortal. *Sci Signal* 2013; **6**: pii.
- Kinoshita T, Hanazawa T, Nohata N *et al.* Tumor suppressive microRNA-218 inhibits cancer cell migration and invasion through targeting laminin-

- 332 in head and neck squamous cell carcinoma. *Oncotarget* 2012; **3**: 1386–400.
- 28 Kinoshita T, Nohata N, Hanazawa T *et al.* Tumour-suppressive microRNA-29s inhibit cancer cell migration and invasion by targeting laminin-integrin signalling in head and neck squamous cell carcinoma. *Br J Cancer* 2013; **109**: 2636–45.
- 29 Nishikawa R, Chiyomaru T, Enokida H *et al.* Tumour-suppressive microRNA-29s directly regulate LOXL2 expression and inhibit cancer cell migration and invasion in renal cell carcinoma. *FEBS Lett* 2015; **589**: 2136–45.
- 30 Mizuno K, Seki N, Mataka H *et al.* Tumor-suppressive microRNA-29 family inhibits cancer cell migration and invasion directly targeting LOXL2 in lung squamous cell carcinoma. *Int J Oncol* 2016; **48**: 450–60.
- 31 Kurozumi A, Kato M, Goto Y *et al.* Regulation of the collagen cross-linking enzymes LOXL2 and PLOD2 by tumor-suppressive microRNA-26a/b in renal cell carcinoma. *Int J Oncol* 2016; **48**: 1837–46.
- 32 Fukumoto I, Kikkawa N, Matsushita R *et al.* Tumor-suppressive microRNAs (miR-26a/b, miR-29a/b/c and miR-218) concertedly suppressed metastasis-promoting LOXL2 in head and neck squamous cell carcinoma. *J Hum Genet* 2016; **61**: 109–18.
- 33 Kamikawaji K, Seki N, Watanabe M *et al.* Regulation of LOXL2 and SERPINH1 by antitumor microRNA-29a in lung cancer with idiopathic pulmonary fibrosis. *J Hum Genet* 2016; **61**: 985–93.
- 34 Kato M, Kurozumi A, Goto Y *et al.* Regulation of metastasis-promoting LOXL2 gene expression by antitumor microRNAs in prostate cancer. *J Hum Genet* 2017; **62**: 123–32.
- 35 Moon HJ, Finney J, Ronnebaum T, Mure M. Human lysyl oxidase-like 2. *Bioorg Chem* 2014; **57**: 231–41.
- 36 Millanes-Romero A, Herranz N, Perrera V *et al.* Regulation of heterochromatin transcription by Snail1/LOXL2 during epithelial-to-mesenchymal transition. *Mol Cell* 2013; **52**: 746–57.
- 37 Mataka H, Seki N, Mizuno K *et al.* Dual-strand tumor-suppressor microRNA-145 (miR-145-5p and miR-145-3p) coordinately targeted MTDH in lung squamous cell carcinoma. *Oncotarget* 2016; **7**: 72084–98.
- 38 Matsushita R, Yoshino H, Enokida H *et al.* Regulation of UHRF1 by dual-strand tumor-suppressor microRNA-145 (miR-145-5p and miR-145-3p): Inhibition of bladder cancer cell aggressiveness. *Oncotarget* 2016; **7**: 28460–87.
- 39 Yonemori M, Seki N, Yoshino H *et al.* Dual tumor-suppressors miR-139-5p and miR-139-3p targeting matrix metalloprotease 11 in bladder cancer. *Cancer Sci* 2016; **107**: 1233–42.
- 40 Matsushita R, Seki N, Chiyomaru T *et al.* Tumour-suppressive microRNA-144-5p directly targets CCNE1/2 as potential prognostic markers in bladder cancer. *Br J Cancer* 2015; **113**: 282–9.
- 41 Byrnes KA, Phatak P, Mansour D *et al.* Overexpression of miR-199a-5p decreases esophageal cancer cell proliferation through repression of mitogen-activated protein kinase kinase-11 (MAP3K11). *Oncotarget* 2016; **7**: 8756–70.
- 42 Gui R, Huang R, Zhang JH, Wen XH, Nie XM. MicroRNA-199a-5p inhibits VEGF-induced tumorigenesis through targeting oxidoreduced-nitro domain-containing protein 1 in human HepG2 cells. *Oncol Rep* 2016; **35**: 2216–22.
- 43 Zhou M, Wang S, Hu L, Liu F, Zhang Q, Zhang D. miR-199a-5p suppresses human bladder cancer cell metastasis by targeting CCR7. *BMC Urology* 2016; **16**: 64.
- 44 Gao Y, Feng Y, Shen JK *et al.* CD44 is a direct target of miR-199a-3p and contributes to aggressive progression in osteosarcoma. *Sci Rep* 2015; **5**: 11365.
- 45 Liu R, Liu C, Zhang D *et al.* miR-199a-3p targets stemness-related and mitogenic signaling pathways to suppress the expansion and tumorigenic capabilities of prostate cancer stem cells. *Oncotarget* 2016; **7**: 56628–42.
- 46 Garzia L, Andolfo I, Cusanelli E *et al.* MicroRNA-199b-5p impairs cancer stem cells through negative regulation of HES1 in medulloblastoma. *PLoS ONE* 2009; **4**: e4998.
- 47 Fang C, Zhao Y, Guo B. MiR-199b-5p targets HER2 in breast cancer cells. *J Cell Biochem* 2013; **114**: 1457–63.
- 48 Gilcrease MZ. Integrin signaling in epithelial cells. *Cancer Lett* 2007; **247**: 1–25.
- 49 Ganguly KK, Pal S, Moulik S, Chatterjee A. Integrins and metastasis. *Cell Adh Migr* 2013; **7**: 251–61.
- 50 Ramovs V, Te Molder L, Sonnenberg A. The opposing roles of laminin-binding integrins in cancer. *Matrix Biol* 2016; **57–58**: 213–24.
- 51 Kamoshida G, Matsuda A, Katabami K *et al.* Involvement of transcription factor Ets-1 in the expression of the alpha3 integrin subunit gene. *FEBS J* 2012; **279**: 4535–46.
- 52 Cagnet S, Faraldo MM, Kreft M *et al.* Signaling events mediated by alpha3-beta1 integrin are essential for mammary tumorigenesis. *Oncogene* 2014; **33**: 4286–95.

Supporting Information

Additional Supporting Information may be found online in the supporting information tab for this article:

Fig. S1. (a) *ITGA3* protein expression levels were measured by western blot after 24 h *ITGA3*-expression vector transfection on SAS cells. GAPDH was used as a loading control. (b) *ITGA3* protein expression levels were measured by western blot 48 h after reverse transfection with *miR-199* family and 24 h after forward transfection with the vector control (VC) and *ITGA3* vector on SAS cells. GAPDH was used as a loading control. (c) Cell proliferation was determined using XTT assays 48 h after reverse transfection with *miR-199* family and 24 h after forward transfection with the vector control (VC) and *ITGA3* vector. ** $P = 0.004$